The Journal of Experimental Biology 208, 2641-2652
Published by The Company of Biologists 2005
doi:10.1242/jeb.01686

Does intracellular metabolite diffusion limit post-contractile recovery in burst locomotor muscle?

Stephen T. Kinsey[1,*], Pragyansri Pathi[2], Kristin M. Hardy[1], Amanda Jordan[2] and Bruce R. Locke[2]

[1]*Department of Biology and Marine Biology, University of North Carolina Wilmington, 601 South College Road, Wilmington, NC 28403-5915, USA* and [2]*Department of Chemical and Biomedical Engineering, FAMU-FSU College of Engineering, Tallahassee, FL 32310-6046, USA*

*Author for correspondence (e-mail: kinseys@uncw.edu)

Accepted 12 May 2005

Summary

Post-metamorphic growth in the blue crab entails an increase in body mass that spans several orders of magnitude. The muscles that power burst swimming in these animals grow hypertrophically, such that small crabs have fiber diameters that are typical of most cells (<60 μm) while in adult animals the fibers are giant (>600 μm). Thus, as the animals grow, their muscle fibers cross and greatly exceed the surface area to volume ratio (*SA*:*V*) and intracellular diffusion distance threshold that is adhered to by most cells. Large fiber size should not impact burst contractile function, but post-contractile recovery may be limited by low *SA*:*V* and excessive intracellular diffusion distances. A number of changes occur in muscle structure, metabolic organization and metabolic flux during development to compensate for the effects of increasing fiber size. In the present study, we examined the impact of intracellular metabolite diffusive flux on the rate of post-contractile arginine phosphate (AP) resynthesis in burst locomotor muscle from small and large animals. AP recovery was measured following burst exercise, and these data were compared to a mathematical reaction–diffusion model of aerobic metabolism. The measured rates of AP resynthesis were independent of fiber size, while simulations of aerobic AP resynthesis yielded lower rates in large fibers. These contradictory findings are consistent with previous observations that there is an increased reliance on anaerobic metabolism for post-contractile metabolic recovery in large fibers. However, the model results suggest that the interaction between mitochondrial ATP production rates, ATP consumption rates and diffusion distances yield a system that is not particularly close to being limited by intracellular metabolite diffusion. We conclude that fiber *SA*:*V* and O_2 flux exert more control than intracellular metabolite diffusive flux over the developmental changes in metabolic organization and metabolic fluxes that characterize these muscles.

Key words: muscle fiber, fiber growth, diffusion, metabolic modeling, reaction–diffusion, exercise, metabolism, scaling, crustacean, blue crab, *Callinectes sapidus*, phosphagen, arginine phosphate, mitochondria.

Introduction

The net rate of metabolic processes in cells depends on the competition between the reactivity of the system and the diffusive flow of substrates to the reaction center (Weisz, 1973). For instance, aerobic metabolism depends on the kinetic properties of the mitochondrial enzymes involved in oxidative phosphorylation and on the diffusive flux of substrates such as ADP to the mitochondria. However, most work on aerobic energy metabolism in skeletal muscle has focused only on the catalytic aspects of cellular enzyme systems. This simplification has been based on the reasoning that cellular dimensions tend to be modest (muscle fibers generally range from 10 to 100 μm in diameter; Russell et al., 2000) and intracellular diffusion distances between mitochondria are typically very short in both aerobic and anaerobic skeletal muscle (e.g. Tyler and Sidell, 1984). Thus, diffusion is assumed to be rapid relative to the catalytic capacity of the mitochondria, leading to minimal intracellular gradients in the concentration of metabolites. This approach has been effectively employed to describe some of the major processes of energy metabolism in muscle, and a variety of kinetic models have been developed that closely match experimental data (e.g. Meyer, 1988; Jeneson et al., 1995; Vicini and Kushmerick, 2000; Korzeniewski, 2003).

While the value of purely kinetic analyses of muscle energy metabolism is readily apparent, the conditions under which diffusive flux may be important in either limiting the net rate of aerobic processes or influencing the evolution of metabolic pathways are unresolved (Suarez, 2003). The principal hurdle to understanding the role of diffusion and metabolic organization is that most metabolic measurements constitute weighted-averages over an entire cell or tissue, making it difficult to observe localized intracellular events or concentration gradients. However, several studies that employed reaction–diffusion mathematical modeling of

aerobic metabolism found theoretical evidence for concentration gradients in high-energy phosphate molecules during steady-state contraction in muscle (Mainwood and Rakusan, 1982; Meyer et al., 1984; Hubley et al., 1997; Aliev and Saks, 1997; Kemp et al., 1998; Vendelin et al., 2000; Saks et al., 2003). The intracellular diffusive flux of high-energy phosphates is largely mediated by phosphagen kinases, such as creatine kinase (CK) and arginine kinase (AK), although the mechanistic details are still the subject of study (reviewed by Walliman et al., 1992; Ellington, 2001).

In an effort to understand the role of diffusion and metabolic organization on the control of metabolism, we have been examining metabolic processes in an extreme anaerobic muscle model system. The muscles that power burst swimming in the blue crab, *Callinectes sapidus*, grow hypertrophically, and during post-metamorphic development the diameter of fibers increases from <60 μm in juveniles to >600 μm in adults (Boyle et al., 2003). Moreover, the distribution of mitochondria changes dramatically during development. In small anaerobic fibers, mitochondria are uniformly distributed throughout the cell, whereas in large fibers the mitochondria are largely clustered at the sarcolemmal membrane, forming an oxidative cylinder at the periphery of the cell (Boyle et al., 2003). Thus, the average distance between mitochondria in small fibers is several microns, while in large fibers there may be hundreds of microns between mitochondrial clusters. The potentially limiting rate of diffusive flux of metabolites over such large distances is exacerbated by intracellular barriers in muscle that lead to a time-dependent reduction in metabolite diffusion coefficients for movement in the direction perpendicular to the fiber axis ($D_{\perp}$) (Kinsey et al., 1999; De Graaf et al., 2001; Kinsey and Moerland, 2002). This means that over the short diffusion distances characteristic of small anaerobic fibers, the $D_{\perp}$ is about 2-fold higher than the $D_{\perp}$ for the long diffusion distances that typify large fibers. While the burst contraction function of these muscles should not be impacted by intracellular diffusion, the aerobic recovery process may be compromised by the extreme size of the fibers in adult animals. There are, in fact, substantial size-dependent differences in the recovery of the anaerobic fibers following burst contraction. Small anaerobic fibers accumulate lactate and modestly deplete glycogen during burst contraction, and both of these metabolites recover to resting levels relatively quickly following an exercise bout (Boyle et al., 2003; Johnson et al., 2004). The large fibers similarly accumulate lactate and deplete glycogen during contraction, but following exercise they continue to accumulate large amounts of lactate and further deplete glycogen. Full aerobic recovery of these metabolites requires several hours in adult blue crabs (Milligan et al., 1989; Henry et al., 1994; Boyle et al., 2003; Johnson et al., 2004).

We have previously hypothesized that anaerobic metabolism is recruited following burst contractions in the large anaerobic fibers to accelerate certain key phases of recovery that would otherwise be overly slow due to intracellular diffusion constraints (Kinsey and Moerland, 2002; Boyle et al., 2003; Johnson et al., 2004). In the present study, we tested this hypothesis by examining the fiber size dependence of the rate of post-contractile arginine phosphate (AP) resynthesis, and these data were compared to a mathematical reaction–diffusion model of aerobic metabolism in crab fibers. The phosphagen, AP, is the initial energy source used during burst contraction, and its rapid resynthesis following an initial exercise bout allows subsequent high-force contractions. We predicted (1) that the measured rate of AP resynthesis would be independent of fiber size, (2) that the predicted rate of AP resynthesis by aerobic metabolism would be fiber size dependent, with a considerably lower rate in large fibers than in small fibers, and (3) that the contributions of anaerobic metabolism would offset intracellular diffusive flux limitations on AP recovery in the large fibers, which would account for the expected contradictory results of (1) and (2) above. Our results were consistent with these predictions, with the exception that intracellular metabolite diffusion does not appear to be a substantial limiting factor of AP recovery rate in large fibers. This suggests that the low fiber surface area:volume ratio (*SA*:*V*), which may limit oxygen flux, is a more important determinant of metabolic rate and/or metabolic design in the large fibers.

Materials and methods

Animals

Juvenile blue crabs (*Callinectes sapidus* Rathbun) were collected by sweep netting in the basin of the Cape Fear River Estuary, NC, USA. Adult crabs were obtained from baited crab traps set in Masonboro Sound, NC, USA or purchased from local fisherman (Wilmington, NC, USA). Crabs were maintained in full-strength filtered seawater (35‰ salinity, 21°C) in aerated, recirculating aquariums. They were fed bait shrimp three times weekly and kept on a 12 h:12 h light:dark cycle. All animals were acclimated for at least 72 h and starved for 24 h before experimental use. Animals were sexed and weighed and their carapace width and body mass were measured prior to use. Only animals in the intermolt stage were used, as determined by the rigidity of the carapace, the presence of the membranous layer of the carapace and the absence of a soft cuticle layer developing beneath the existing exoskeleton.

Exercise protocol

Crabs were induced to undergo a burst swimming response as described previously (Boyle et al., 2003; Johnson et al., 2004). Crabs were held suspended in the air by a clamp in a manner that allows free motion of the swimming legs, and small wire electrodes were placed in two small holes drilled into the mesobranchial region of the dorsal carapace. A Grass Instruments SD9 physiological stimulator (Astro Med, Inc., West Warwick, RI, USA) was used to deliver a small voltage (80 Hz, 200 ms duration, 10 V cm^{-1} between electrodes) to the thoracic ring ganglia, which elicited a burst swimming response in the 5th periopods for several seconds following the stimulation. A single pulse was administered every 30 s until the animal was no longer capable of a burst response, which was evident when it responded by moving its legs at a notably slower rate. Immediately

following exercise, animals were returned to aerated full-strength seawater for a recovery period of 0, 15, 30 or 60 min.

Metabolite measurement

At the end of the recovery period, crabs were rapidly cut in half along their sagittal plane in order to minimize spontaneous burst contraction of the swimming legs that typically occurs during sacrifice. The dorsal carapace, reproductive and digestive organs were removed and the basal cavity, which houses the muscles of the fifth periopod, was exposed. The light levator muscle was rapidly isolated by cutting away the surrounding muscle and freeze-clamped while still intact within the animal. The time elapsed from sacrifice to freeze clamping the muscle was 60–90 s. Tissue samples were immediately homogenized in a 6–35-fold dilution of chilled 7% perchloric acid with 1 mmol EDTA using a Fisher Powergen 125 homogenizer and then centrifuged at 16 000 ***g*** for 30 min at 4°C. The supernatant pH was neutralized with 3 mol l^{-1} potassium bicarbonate in 50 mmol l^{-1} PIPES, stored on ice for 10 min and centrifuged at 16 000 ***g*** for 15 min at 4°C. The supernatant was immediately analyzed by ^{31}P nuclear magnetic resonance (NMR) spectroscopy. NMR spectra were collected at 162 MHz on a Bruker 400 DMX spectrometer to determine relative concentrations of AP and inorganic phosphate (P_i). Spectra were collected using a 90° excitation pulse and a relaxation delay of 12 s, which ensured that the phosphorus nuclei were fully relaxed and peak integrals for the metabolites were proportional to their relative concentrations. Forty-eight scans were acquired for a total acquisition time of 10 min. The area under each peak was integrated using Xwin-NMR software to yield relative concentrations of each metabolite. Two-way analysis of variance (ANOVA) was used to analyze the post-contractile metabolite concentrations for the interaction between size class and recovery time. All metabolite data are presented as means ± S.E.M.

Mathematical modeling

The general modeling approach was the same as that described in Hubley et al. (1997), with parameters adjusted to comply with blue crab fibers and the addition of a mitochondrial reaction boundary condition, a basal rate of ATP consumption, an appropriate kinetic expression for the phosphagen kinase (AK), and $D_\perp$ values from crustacean anaerobic fibers that incorporated the time dependence of diffusion (Kinsey and Moerland, 2002). The diffusion and reaction of ATP, ADP, AP, arginine (Arg) and P_i were modeled in a one-dimensional system that extended from the surface of a mitochondrion to a distance ($\lambda/2$) equal to half of the mean free spacing between mitochondria or between clusters of mitochondria. Reactions catalyzed by AK, myosin ATPase and basal ATPase were assumed to occur homogenously throughout the domain $0 \leqslant x \leqslant \lambda/2$, where x is distance from the mitochondrial surface. A burst contraction–recovery cycle was modeled in the anaerobic, light levator fibers (so named because they lack the high density of mitochondria that give the aerobic, dark levator its characteristic pigmentation; Tse et al., 1983) using conditions appropriate for a small (100 μm)-diameter fiber from a juvenile animal and a large (600 μm)-diameter fiber from an adult. Simulations were generated using the finite element analysis software, FEMLAB (Comsol, Inc., Burlington, MA, USA).

Temporally and spatially dependent concentration profiles of ATP, ADP, AP, Arg and P_i were calculated according to the molar-species continuity equation:

$$\frac{\partial C_i}{\partial t} = D_{\perp i}\frac{\partial^2 C_i}{\partial x^2} + R_i \ , \qquad (1)$$

where C_i is the molar concentration of species i (ATP, ADP, AP, Arg, P_i) and t is time. R_i is the sum of the reaction rates in the intermitochondrial 'bulk' space in which species i participates and includes the basal ATP consumption, myosin ATPase and AK. The initial conditions were $C_i = C_i^0$ over the domain $0 \leqslant x \leqslant \lambda/2$ at $t=0$, where C_i^0 is the resting concentration of species i.

The mitochondrial boundary conditions at $x=0$ balance the fluxes of ATP and ADP into the bulk phase with the rates of formation and consumption at the mitochondria and are modeled using Michaelis-Menten kinetics with ADP activation (Meyer et al., 1984):

$$R_{ATP}^{mito} = D_{\perp ATP}\frac{\partial C_{ATP}}{\partial x} = \frac{V_{m,mito}\cdot C_{ADP}}{K_{m,mito}+C_{ADP}} \ , \qquad (2)$$

$$R_{ADP}^{mito} = D_{\perp ADP}\frac{\partial C_{ADP}}{\partial x} = -\frac{V_{m,mito}\cdot C_{ADP}}{K_{m,mito}+C_{ADP}} \ , \qquad (3)$$

where R_{ATP}^{mito} and R_{ADP}^{mito} are the boundary reaction rates for ATP and ADP, respectively, $V_{m,mito}$ is the maximal velocity (V_{max}) of the boundary reaction, and $K_{m,mito}$ is the Michaelis constant for ADP for the boundary reaction. While there is considerable evidence for more complex control of mitochondrial ATP production (e.g. Korzeniewski, 2003), even when considering ADP as the sole activating species (Jeneson et al., 1996), we have used the simplified approach described here because the mitochondrial reaction will be functioning near $V_{m,mito}$ during most of recovery, making a detailed kinetic mechanism describing oxidative phosphorylation (which is lacking for crustacean muscle) unnecessary to achieve our objectives. There are no fluxes of Arg, AP or P_i into the bulk phase since these species do not participate in the mitochondrial reaction:

$$\frac{\partial C_{AP}}{\partial x} = \frac{\partial C_{Arg}}{\partial x} = \frac{\partial C_{Pi}}{\partial x} = 0 \ . \qquad (4)$$

A basal ATPase rate in the bulk phase was modeled using an equation of the same form as for the mitochondrial boundary reaction (Eqn 2), and the basal reaction values $V_{m,bas}$ and $K_{m,bas}$ were adjusted to maintain C_i^0 constant over time in inactive fibers and to promote a return to the initial steady state following metabolic recovery. No-flux boundary conditions ($dC_i/dx=0$) were also applied for all species at $x=\lambda/2$ to provide symmetry about this boundary.

AK catalyzes the reversible phosphoryl-transfer reaction AP+ADP↔Arg+ATP, and intracellular AP serves as the initial energy source used during burst contraction in crustacean muscle. The reaction proceeds by a rapid equilibrium, random mechanism and was modeled according to the kinetic

expression of Smith and Morrison (1969):

$$R_{ATP}^{AK} = \frac{V_{m,AK,rev}C_{ATP}C_{Arg} - V_{m,AK,for}\frac{K_{i,ATP}K_{i,Arg}}{K_{m,AP}K_{i,ADP}}C_{AP}C_{ADP}}{K_{i,ATP}K_{m,Arg}+K_{m,ATP}C_{Arg}+K_{m,Arg}C_{ATP}+C_{ATP}C_{Arg}+\frac{K_{i,ATP}K_{m,Arg}C_{AP}}{K_{i,AP}}+\frac{K_{i,ATP}K_{m,Arg}C_{ADP}}{K_{i,ADP}} + \frac{K_{i,ATP}K_{m,Arg}C_{AP}C_{ADP}}{K_{i,AP}K_{i,ADP}}+\frac{K_{i,ATP}K_{m,Arg}C_{ATP}C_{Arg}}{K_{i,ATP}K_{i,AP}}+\frac{K_{i,ATP}K_{m,Arg}C_{Arg}C_{ADP}}{K_{i,Arg}K_{i,ADP}}}, \quad (5)$$

where $V_{m,AK,for}$ and $V_{m,AK,rev}$ are V_{max} values in the forward (ATP formation) and reverse direction, respectively, K_m values are Michaelis constants for ternary complex formation, K_i values are free enzyme–substrate complex dissociation constants, K_I values are dissociation constants relevant to the formation of dead-end complexes, and $R_{ATP}^{AK}=-R_{ADP}^{AK}=-R_{AP}^{AK}=R_{Arg}^{AK}$.

Myosin ATPase was modeled using Michaelis-Menten kinetics (Pate and Cooke, 1985; Hubley et al., 1997):

$$R_{ATP}^{myo} = -\frac{V_{m,myo}\cdot C_{ATP}}{K_{m,myo}+C_{ATP}}, \quad (6)$$

where $V_{m,myo}$ is the V_{max}, $K_{m,myo}$ is the apparent Michaelis constant for ATP, and $R_{ATP}^{myo}=-R_{ADP}^{myo}=-R_{Pi}^{myo}$.

For each simulation, myosin ATPase was activated for 7 s at 10 Hz to simulate burst contraction and was then deactivated during the post-contractile recovery period, whereas the basal ATPase was active throughout the entire contraction–recovery cycle. Small fibers (100 μm diameter) were modeled assuming a uniform distribution of mitochondria, whereas large fibers (600 μm diameter) were assumed to have mitochondria only at the periphery of the fiber (subsarcolemmal mitochondria) as described in Boyle et al. (2003). Large fibers were also modeled assuming a uniform distribution of mitochondria in order to assess the consequences of the extreme diffusion distances (300 μm) associated with an exclusively subsarcolemmal distribution.

Model input parameters are detailed in Table 1. The resting metabolite concentrations for crustacean anaerobic locomotor fibers were obtained from a combination of the data in Head and Baldwin (1986), ^{31}P-NMR spectra collected by Kinsey and Ellington (1996) and calculations using the AK equilibrium constant (Teague and Dobson, 1999). The resting metabolite concentrations were the same in small and large fibers (Baldwin et al., 1999). The $D_\perp$ values for each metabolite were based both on direct measurements from crustacean anaerobic fibers and calculations from the relationship of molecular mass and $D_\perp$ in these fibers (Kinsey and Moerland, 2002). The $D_\perp$ used for the short diffusion distances characteristic of small fibers was higher than that for the long distances found in large fibers due to the time dependence of radial diffusion in muscle (Kinsey et al., 1999; Kinsey and Moerland, 2002). Intracellular diffusion distances (λ/2) were estimated from the total mitochondrial fractional area (A_{mito}/A_{cell}), which was 0.026 in small fibers and 0.017 in large fibers (recalculated from data collected by Boyle et al., 2003), and the mean area/mitochondrion (a_{mito}), which was 0.608 μm^2 (Boyle et al., 2003), using the relationship:

$$\lambda/2 = \sqrt{\frac{a_{mito}}{A_{mito}/A_{cell}}\times\frac{1}{\pi}}. \quad (7)$$

The $V_{m,mito}$ values were estimated from rates of aerobic post-contractile phosphagen resynthesis from white muscle fibers with a mitochondrial density comparable to blue crab light levator muscle. Data from small prawn anaerobic tail muscle that would not be expected to have large fibers (Thébault et al., 1987) and from isolated dogfish white muscle, which resynthesizes phosphocreatine (PCr) using only aerobic metabolism and has a mitochondrial fractional area of ~0.01 (Curtin et al., 1997), yielded very similar estimates for $V_{m,mito}$. This approach was necessary due to an absence of suitable measurements of maximal oxygen consumption or ATP production rates from isolated crustacean anaerobic fibers and because estimates of $V_{m,mito}$ derived from mammalian studies (corrected for differences in mitochondrial density) yielded AP recovery rates that were several-fold higher than those observed in the literature or presented here. This is consistent with the fact that phosphagen recovery rates in mammalian muscle (e.g. Vicini and Kushmerick, 2000) are >10-fold higher than rates in crustacean muscle (Thébault et al., 1987). Rates of mitochondrial ATP production per cell volume were converted to rates of flux per mitochondrial surface area using a mitochondrial *SA*:*V* ratio of 6.81 and the mitochondrial fractional area data for small and large levator fibers (Boyle et al., 2003). A $K_{m,mito}$ value for ADP of 20 μmol l^{-1} was used, which is within the range for fast skeletal muscle (Meyer et al., 1984). AK dissociation constants were obtained from Smith and Morrison (1969), $V_{m,AK,rev}$ was taken from Zammitt and Newsholme (1976) and $V_{m,AK,for}$ was calculated from the AK Haldane relationship from Smith and Morrison (1969) using an equilibrium constant for AK of 39 (Teague and Dobson, 1999). Values for $V_{m,myo}$ and $K_{m,myo}$ were the same as in Hubley et al. (1997).

While the model generated temporally and spatially resolved concentrations of metabolites, our experimental measurements yielded values that were spatially averaged across the fiber. In order to compare the model results with the experimental data,

Table 1. *Parameters used in reaction–diffusion model*

Parameter type	Parameter	Value small fiber	Value large fiber	Units
Initial concentrations	AP	34.3	34.3	mmol l^{-1}
	Arginine	0.47	0.47	mmol l^{-1}
	P_i	4.88	4.88	mmol l^{-1}
	ATP	8.6	8.6	mmol l^{-1}
	ADP	0.01	0.01	mmol l^{-1}
Diffusion	$D_{\perp,AP}$	2.20 10^{-6}	1.00 10^{-6}	cm^2 s^{-1}
	$D_{\perp,Arg}$	2.79 10^{-6}	1.27 10^{-6}	cm^2 s^{-1}
	$D_{\perp,Pi}$	3.56 10^{-6}	1.62 10^{-6}	cm^2 s^{-1}
	$D_{\perp,ATP}$	1.54 10^{-6}	0.70 10^{-6}	cm^2 s^{-1}
	$D_{\perp,ADP}$	1.75 10^{-6}	0.79 10^{-6}	cm^2 s^{-1}
	$\lambda/2$	2.73	300	μm
Mitochondrial boundary reaction	$V_{m,mito}$	3.40	2.22	μmol l^{-1} s^{-1}
	$K_{m,mito}$	20	20	μmol l^{-1}
Basal ATPase	$V_{m,bas}$	11.75	11.75	μmol l^{-1} s^{-1}
	$K_{m,bas}$	100	100	mmol l^{-1}
Arginine kinase reaction	$V_{m,AK,for}$	611	611	mmol l^{-1} s^{-1}
	$V_{m,AK,rev}$	39	39	mmol l^{-1} s^{-1}
	K_{ATP}	0.32	0.32	mmol l^{-1}
	K_{Arg}	0.75	0.75	mmol l^{-1}
	K_{AP}	3.82	3.82	mmol l^{-1}
	K_{ADP}	0.40	0.40	mmol l^{-1}
	$K_{i,ATP}$	0.34	0.34	mmol l^{-1}
	$K_{i,Arg}$	0.81	0.81	mmol l^{-1}
	$K_{i,AP}$	0.26	0.26	mmol l^{-1}
	$K_{i,ADP}$	0.024	0.024	mmol l^{-1}
	$K_{I,ATP}$	2.43	2.43	mmol l^{-1}
	$K_{I,Arg}$	3.45	3.45	mmol l^{-1}
Myosin ATPase	$V_{m,myo}$	6.92	6.92	mmol l^{-1} s^{-1}
	$K_{m,myo}$	0.15	0.15	mmol l^{-1}

See text for additional details and source information.

some of the model data were mathematically volume averaged over the domain from x=0 to x=λ/2:

$$<C_i(t)> = \frac{\int_{x=0}^{x=\lambda/2} C_i(x,t)\,dx}{\lambda/2} \quad . \qquad (8)$$

For model simulations that were volume averaged, the duration of myosin ATPase activation was adjusted so that the decrease in [AP] was comparable to that in the observed data, in order to facilitate comparison of AP recovery measurements with the model.

Results

Arginine phosphate recovery

Crab body mass for the small size class had a median value of 1.6 g and a range from 0.7 to 3.5 g (N=40), while the large size class had a median of 184.5 g and a range from 89.0 to 285.0 g (N=53). This corresponds to an estimated median fiber size in the light levator muscle of the small size class of 131 μm, with a range from 54 to 221 μm, and in the large size class of 607 μm, with a range from 433 to 770 μm (fiber sizes estimated from data summarized in Boyle et al., 2003). The crab stimulation procedure elicited a burst exercise response that was qualitatively similar among the two size classes, as reported previously (Boyle et al., 2003; Johnson et al., 2004). While the frequency of swimming leg movement was higher in the juvenile animals, the duration of swimming was greater in the adult animals. However, the AP depletion (see below), glycogen depletion (Boyle et al., 2003) and lactate accumulation (Johnson et al., 2004) during exercise were identical in muscle fibers from the juvenile and adult crabs, indicating that the metabolic effects of exercise on the muscle were the same in both size classes.

Examples of ^{31}P-NMR spectra from perchloric acid muscle extracts demonstrate the reciprocal change of AP and P_i during a burst exercise–recovery cycle that results from the stoichiometric coupling of cellular ATPases (including myosin ATPase) and the AK reaction (Fig. 1). The time course of relative changes in AP and P_i concentrations is shown in Fig. 2, where the NMR peak integrals at each time point have been normalized to the mean resting integrals to allow direct comparison of the rate of recovery in small and large animals. A rapid depletion of AP (and increase in P_i) is followed in small and large fibers by a slow recovery that is complete in

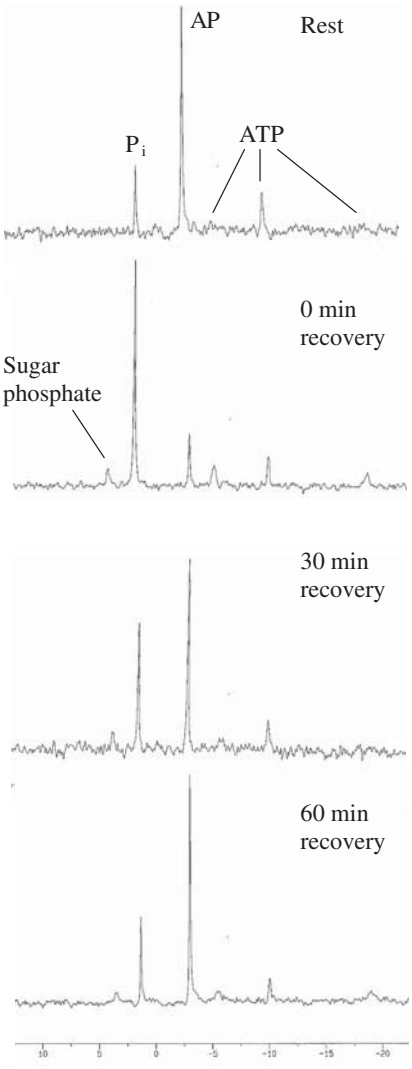

Fig. 1. Representative ^{31}P-NMR spectra collected from perchloric acid extracts of large light levator muscle fibers that demonstrate the changes in relative concentrations of AP and P_i during a contraction–recovery cycle. Spectra were collected from crabs at rest and after 0, 30 and 60 min of recovery from burst exercise. Chemical shifts are in units of parts per million.

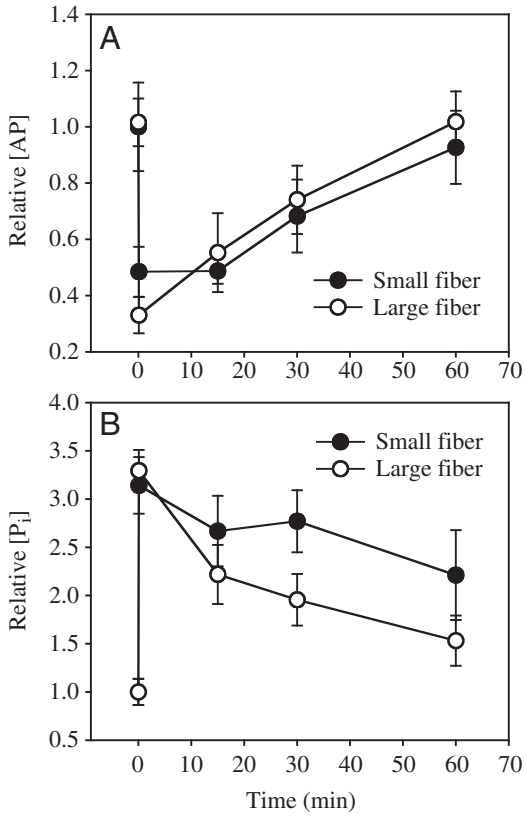

Fig. 2. Relative changes in (A) AP and (B) P_i concentrations in small (filled symbols) and large (open symbols) light levator fibers during a contraction–recovery cycle. $N \geqslant 5$ for every point.

about 60 min. Despite the large differences in body mass and fiber size between the small and large animals, the rate of recovery was essentially the same for both groups and there was no significant interaction between size class and recovery time for AP (F=0.63, d.f.=3, P=0.60) or P_i (F=1.78, d.f.=3, P=0.16).

Reaction–diffusion analysis of contraction and recovery

Since the size independence of post-contractile AP resynthesis described above presumably arises from anaerobic contributions to recovery in the large fibers (Boyle et al., 2003; Johnson et al., 2004), the reaction–diffusion analysis allows us to test whether this pattern results from diffusive constraints on the aerobic component of recovery. The spatially and temporally resolved concentrations of high-energy phosphate molecules are presented in Fig. 3. The rate of recovery was somewhat faster in the small than in the large fibers, and there were no intracellular gradients in small fibers, as expected. However, there were only mild gradients present in the large fibers, indicating that diffusive flux is fast relative to the mitochondrial reaction (Fig. 3). This result is not consistent with intracellular diffusive flux limiting aerobic metabolism during post-contractile recovery, even though metabolite diffusion in the large fiber was modeled over a distance of 300 μm. Thus, the relatively small differences between the small and large fibers in Fig. 3 result almost exclusively from differences in mitochondrial density (Table 1). The model results were also volume-averaged to allow a comparison of the observed and simulated recovery rates. The observed and modeled AP recovery data are in agreement for the small fibers, but in the large fibers it is clear that aerobic metabolism alone could not account for the relatively high observed rate of post-contractile recovery (Fig. 4). Thus, anaerobic metabolism appears to accelerate AP recovery in the large fibers, but in the context of the present model this simply serves to offset the mass-specific decrease in aerobic capacity that typifies metabolic scaling in general (Schmidt-Nielson, 1984) and not to compensate for diffusion limitations.

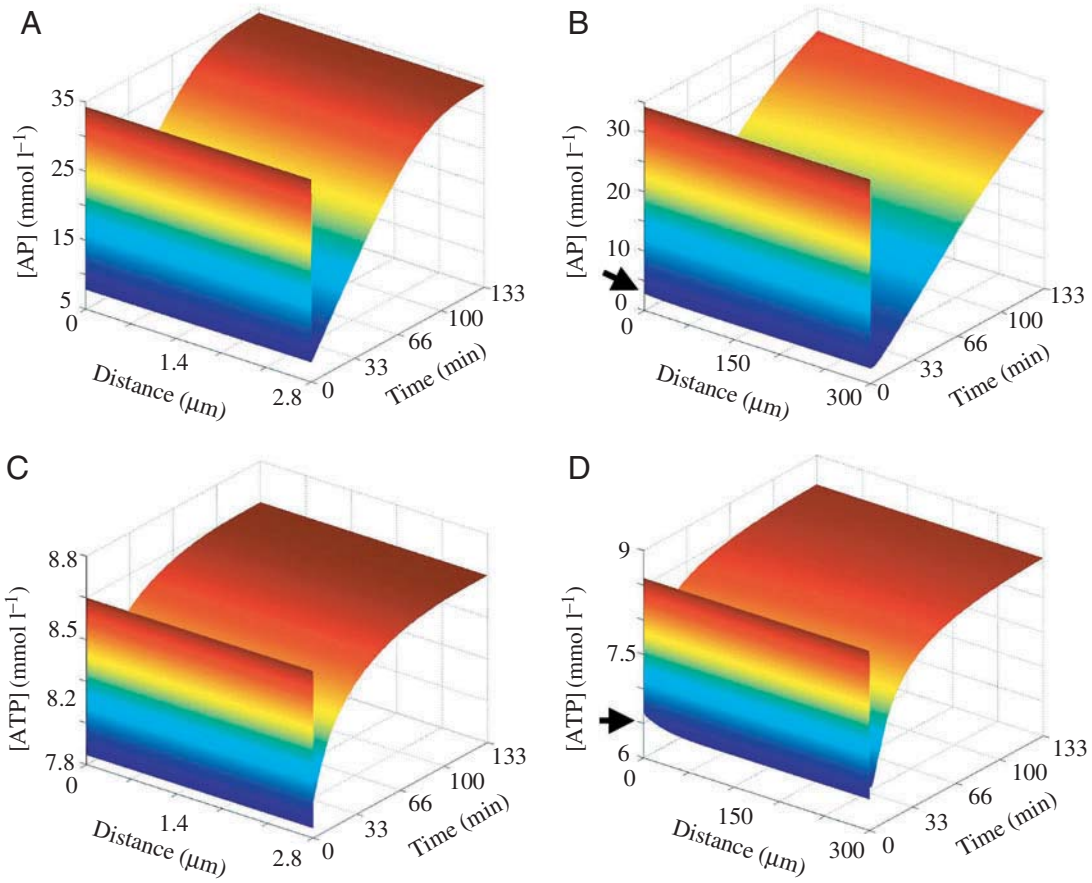

Fig. 3. Model output for small (A,C) and large (B,D) light levator fibers using parameters in Table 1. The small fibers were modeled assuming a uniform distribution of mitochondria, while the large fibers were modeled assuming only subsarcolemmal mitochondria (Boyle et al., 2003). The temporally and spatially resolved concentrations of AP and ATP during a contraction–recovery cycle are shown. The arrows indicate where mild gradients exist in the large fibers. For AP, the gradients are not obvious due to the scaling of the concentration axis, but they are of a magnitude similar to that seen in ATP. ADP, Arginine and P_i are not shown, but the concentrations change in reciprocal fashion to that of AP.

If recovery in the large fibers is not substantially constrained by diffusion, then how close are the fibers to being limited by intracellular diffusive flux? Fig. 5 shows the effect of incremental increases in the rate of the mitochondrial boundary reaction. It can be seen that doubling the $V_{m,mito}$ leads to the formation of only slightly steeper concentration gradients, which means that there is a minimally increased control of aerobic flux by intracellular diffusion, and the concentration gradients grow more substantial as $V_{m,mito}$ is further increased. However, it is also clear that the metabolic recovery rate increases in proportion to the increases in $V_{m,mito}$. Only when unrealistically high rates of $V_{m,mito}$ are used do steep concentration gradients appear, indicating diffusion limitation of recovery rate. Thus, the mitochondrial reaction rate used in the model fits our data well (Fig. 4) and is considerably below that which would lead to substantial diffusive limitations of aerobic flux in large fibers (Fig. 5).

In the simulations of the large light levator fibers, we have assumed that all of the mitochondria are subsarcolemmal, which is consistent with the dramatic shift of mitochondrial distribution toward the fiber periphery during development (Boyle et al., 2003). To assess the impact of this reorganization of mitochondria during development, we also analyzed the large fibers, assuming a uniform distribution of mitochondria similar to that seen in the small fibers. The mean λ/2 value calculated from the total mitochondrial fractional area from large fibers was 3.4 μm, which is only slightly greater than in small fibers (Table 1) but nearly two orders of magnitude less than for the exclusively subsarcolemmal distribution assumed in Figs 3–5. Despite the large difference in diffusion distance, the rate of metabolic recovery assuming a uniform distribution of mitochondria was almost identical to that shown in Fig. 3 (slightly higher), and no concentration gradients were observed (data not shown). This result is also consistent with a very limited control of metabolic flux by intracellular diffusion.

Discussion

The principal findings of the present study were (1) that AP recovery following burst contraction was independent of body mass and fiber size, (2) that the predicted rate of aerobic metabolism was insufficient to account for the relatively high

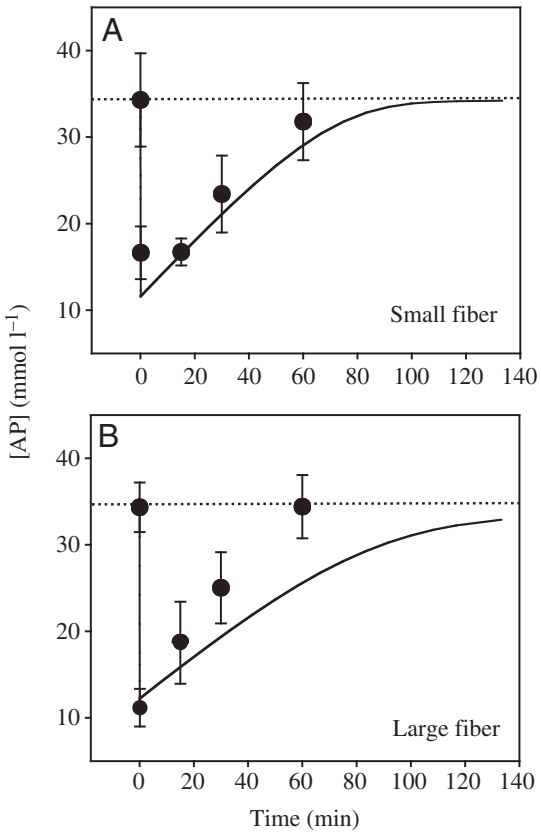

Fig. 4. Measured AP recovery (symbols) compared with the volume-averaged model of AP recovery (solid line) in small (A) and large (B) fibers. The measured AP data have been normalized to a resting concentration of 34.3 mmol l^{-1} to coincide with that of the model. In the model, the myosin ATPase was activated long enough to cause a decrease in AP that was comparable to the measured data. The dotted line indicates the resting concentration.

rate of recovery in the large fibers, which is consistent with the hypothesis that anaerobic metabolism contributes to AP recovery to a greater extent as fibers grow, and (3) that intracellular diffusive flux does not appear to limit metabolic recovery in large fibers, despite the fact that diffusion must occur over hundreds of microns. Rather, the fibers appear to have an aerobic capacity that is considerably below that which would lead to substantial diffusion limitation (Fig. 5).

It is well established that some crustacean muscles produce lactate following contraction, and it has been speculated that this leads to an increased rate of metabolic recovery (Ellington, 1983; Head and Baldwin, 1986; Kamp, 1989; Henry et al., 1994; Baldwin et al., 1999; Morris and Adamczewska, 2002; Johnson et al., 2004). We first described the fiber size-dependence of post-exercise glycogen depletion (Boyle et al., 2003) and lactate production (Johnson et al., 2004) in crustacean muscle and attributed the observed pattern to the long intracellular diffusion distances and/or the low *SA*:*V* associated with the large developmental increase in fiber size. While the studies cited above suggested that post-contractile recovery was accelerated by anaerobic metabolism, the present study is, to our knowledge, the first demonstration in crustacean muscle of a metabolic recovery process (AP resynthesis) that is faster in the large fibers as a result of anaerobic contributions.

In our view, the patterns of recovery reported previously (Boyle et al., 2003; Johnson et al., 2004) and herein are clearly related to fiber size. It was therefore surprising that the model results did not indicate a limitation of aerobic flux by intracellular metabolite diffusion, considering that AP and arginine, which are the key diffusing species (Ellington and Kinsey, 1998), can traverse the $\lambda/2$ distance in small fibers in <30 ms, while needing 16 000 times longer (nearly 8 min) to cover the distance modeled in large fibers (Kinsey and Moerland, 2002). Implicit in this finding is that kinetic expressions alone (no diffusion component) would have been nearly sufficient to simulate the differences between small and large fibers in Fig. 3. This is at odds with some previous reaction–diffusion mathematical analyses in burst anaerobic muscle. Hubley et al. (1997) found substantial concentration gradients for PCr and the free energy of ATP hydrolysis (ΔG_{ATP}) in fish white muscle during contraction, while Boyle et al. (2003) applied the reaction–diffusion model of Mainwood and Rakusan (1982) to blue crab light levator muscle and likewise found dramatic concentration gradients for AP and ΔG_{ATP}. However, both of these models assumed higher rates of steady-state ATP demand and perfect buffering of high-energy phosphate concentrations at the mitochondrial membrane, which means that rates of ATP chemical flux were always high relative to the rates of diffusive flux. By contrast, the present study used a simple kinetic expression for the mitochondrial boundary reaction and reasonable maximal rates of ATP production. Further, no additional ATP demand was applied during recovery beyond the thermodynamic drive to restore the resting steady-state metabolite concentrations.

It could be argued that we underestimated the $V_{m,mito}$ and post-contractile ATP demand and therefore misjudged the effect of diffusion. Thus, the approach used herein represents a conservative analysis of the potential for diffusion limitation in these muscle fibers. It should be noted, however, that the model results for AP recovery paralleled our observations in the small fibers (Fig. 4), which rely exclusively on aerobic metabolism for recovery (Boyle et al., 2003; Johnson et al., 2004), and the low $V_{m,mito}$ values are consistent with observations that complete aerobic recovery from exercise in blue crabs occurs over many hours (Booth and McMahon, 1985; Milligan et al., 1989; Henry et al., 1994; Boyle et al., 2003; Johnson et al., 2004). Our results are also consistent with the generalized analysis of diffusion limitation described by Weisz (1973), which relates the observed rate of the catalytic process to rates of diffusive flux. Applying this approach to the present case, we can conclude that even if $V_{m,mito}$ and post-contractile ATPase rates were underestimated, the observed rate of AP recovery is simply too slow to be limited by diffusive flux (Weisz, 1973).

There are other possible size-dependent effects that could

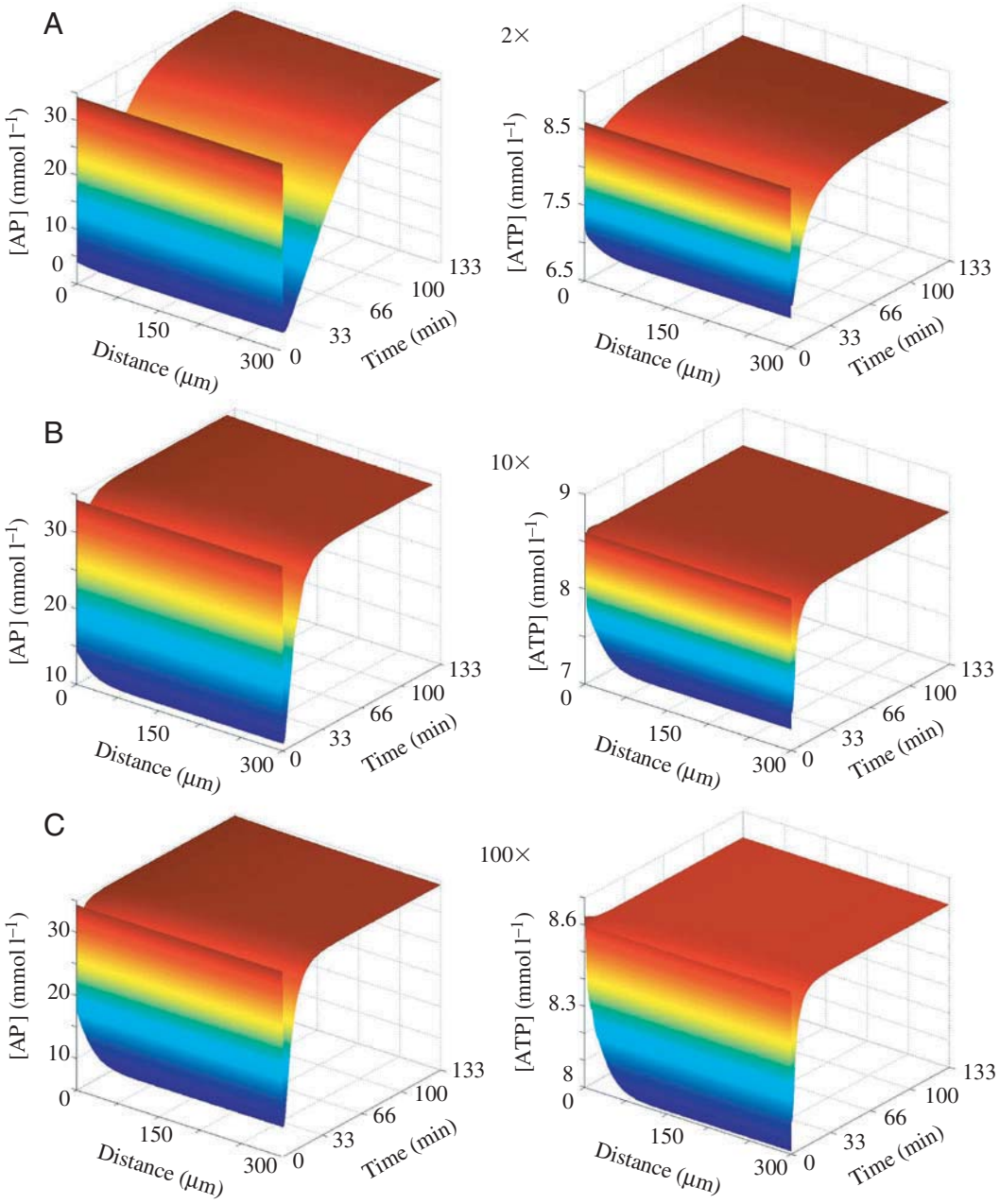

Fig. 5. The effect of increasing the rate of mitochondrial ATP production in large fibers on the temporal and spatial concentration profiles of AP (left panels) and ATP (right panels). All parameters are the same as in Fig. 3B,D, except that the $V_{m,mito}$ has been increased over the value used in Fig. 3 by 2-fold (A), 10-fold (B) and 100-fold (C).

confound our analysis. For instance, size-dependent differences in AP hydrolysis during dissection, freeze clamping or perchloric acid extraction could conceivably bias our AP recovery curves. However, in resting animals, the AP/P_i ratios in extracts were always similar to previous values observed in intact, superfused crustacean white muscle (Kinsey and Ellington, 1996), and there were no significant differences in the AP/P_i ratios between size classes (data not shown). Therefore, AP hydrolysis during the dissection and/or extraction was minimal and not size dependent. It is also possible that differences in intracellular pH (pH_i) or free Mg^{2+} between large and small animals could alter the AK equilibrium constant and therefore the AP recovery rate. While lactate accumulation during contraction is the same in both size classes, post-contractile lactate accumulation is greater in the large fibers (Johnson et al., 2004), and this could lead to a reduced pH_i in large fibers that would slow AP recovery. In addition, the low *SA*:*V* in large fibers may hinder compensatory acid/base equivalent exchange and exacerbate cellular acidosis, again leading to slower AP recovery. However, it should be noted that both the post-contractile lactate production and potential effects of *SA*:*V* still fall within the

realm of fiber size effects, which is consistent with our conclusions. In addition, intracellular buffering capacity in white muscle of crustaceans is greater in larger animals (Baldwin et al., 1999), which may offset the pH_i effects described above.

The findings in the present study are somewhat paradoxical. If it is assumed that a relatively rapid post-contractile recovery in burst muscle is beneficial, which is apparently the case since large fibers use anaerobic metabolism to speed up recovery, and if intracellular diffusive flux does not limit recovery, then why do the large fibers not simply increase the mitochondrial density to accelerate recovery rather than relying on anaerobic processes that put them further in oxygen debt? It is clear from Figs 3 and 5 that doubling the mitochondrial density leads to a near doubling of recovery rate, with only mild limitation by diffusion. We propose that, in blue crabs, the low *SA*:*V* associated with large fiber size is more important in limiting aerobic metabolism and/or driving metabolic design than is intracellular metabolite diffusion. The most compelling evidence in support of this argument is the dramatic shift in the distribution of mitochondria toward the periphery of the fiber as the light levator muscle fibers grow (Boyle et al., 2003). This distributional change places more mitochondria at the sarcolemmal membrane near the source of O_2 at the expense of increased intracellular diffusion distances. In our model analysis, there was a very slight advantage associated with a uniform, instead of subsarcolemmal, distribution of mitochondria in the large fibers (data not shown). However, the fact that the developmental shift in mitochondria occurs anyway indicates that O_2 flux (which was not included in the model) drives mitochondrial distribution more than intracellular diffusive flux. This view has been suggested previously to explain mitochondrial clustering at the sarcolemma in non-giant mammalian (Mainwood and Rakusan, 1982) and crustacean muscle (Stokes and Josephson, 1992).

In addition to the above argument, the partial pressure of oxygen ($\dot{P}_{O_2}$) in crustacean blood (including blue crabs) is low relative to that of muscle from active vertebrate species (Gannon and Wheatly, 1995; Forgue et al., 2001). This leads to relatively shallow $\dot{P}_{O_2}$ gradients across the sarcolemma that, when coupled to the low *SA*:*V* of large fibers, would be expected to promote very low rates of O_2 flux into the fiber. The lack of myoglobin (Mb) in the light levator muscle amplifies this effect, since Mb-less fibers require a higher extracellular $\dot{P}_{O_2}$ to support a given rate of O_2 consumption compared with muscles with Mb (Groebe and Thews, 1990). This view is consistent with recent observations in isolated *Xenopus laevis* skeletal muscle fibers, which are also relatively large and lack Mb, that low intracellular $\dot{P}_{O_2}$ limits the rate of NAD(P)H oxidation by the electron transport system during steady-state contraction (Hogan et al., 2005). Further, the modeled differences between the recovery rate in small and large fibers are modest, due to the relatively small differences in oxidative potential (Figs 3, 4; Table 1), but the measured differences in post-contractile lactate production among size classes are dramatic; far greater than would be necessary to accelerate AP resynthesis by the relatively small amount indicated in Fig. 4 (Johnson et al., 2004). If fiber *SA*:*V* limits aerobic metabolism then the size dependence of aerobic recovery may be much more substantial than is shown in Fig. 3, which would explain the strong size dependence of post-contractile lactate production.

While intracellular diffusive fluxes of high-energy phosphate metabolites do not appear to exert substantial control over the rate of aerobic metabolism in blue crab giant anaerobic fibers, based on our current one-dimensional model, there may be other cell types where diffusion is limiting. These are likely to include systems with relatively high rates of ATP production/consumption and distant sites of ATP utilization, such as in some muscle fibers with a higher aerobic capacity than examined here (Meyer et al., 1984; Stokes and Josephson, 1992; Vendelin et al., 2000; Saks et al., 2003; Suarez, 2003) or in the flagellum of spermatozoa, which has been the subject of many reaction–diffusion analyses (e.g. Nevo and Rikmenspoel, 1969; Tombes and Shapiro, 1985; Van Dorsten et al., 1997; Ellington and Kinsey, 1998). However, it is possible that in most cases neither intracellular metabolite diffusion nor sarcolemmal O_2 flux limit aerobic metabolism *per se*, but even if this is true it is still likely that the interaction between diffusive processes and ATP demand has shaped the evolution of cellular design. For instance, if there are advantages to having large fibers then the principles of symmorphosis (Taylor and Weibel, 1981) dictate that other metabolic properties, such as mitochondrial density and distribution, would be adjusted to match rates of O_2 and substrate delivery, thereby avoiding diffusion limitation.

What then are the potential advantages associated with large muscle fibers? Rome and Lindstedt (1998) have characterized the manner in which muscle fiber volume is devoted to metabolic or contractile machinery in relation to muscle function. It is possible that a burst contractile muscle composed of relatively few large fibers may yield a greater percentage of total muscle volume that is devoted to myofibrils, and therefore improve contractile force, compared with muscle with a much larger number of small fibers. Johnston et al. (2003, 2004) proposed that in certain cold-water fishes white muscle fibers attain a size that is just below that which would be diffusion-limited in order to minimize sarcolemmal surface area over which ionic gradients must be maintained, thus lowering metabolic rates. A similar argument could be made for blue crab anaerobic fibers, with the additional consideration that a low mitochondrial content may also constitute an energy-saving strategy to avoid the costs of mitochondrial biogenesis and the maintenance of electrochemical gradients across the inner membrane. Forgue et al. (2001) have made complimentary arguments that the low blood $\dot{P}_{O_2}$ in crustaceans limits resting metabolic rate to reduce costs during periods of inactivity. These proposed energy-saving measures are linked; if the capacity to produce ATP is strategically lowered, then there is no negative consequence to the low *SA*:*V* and long diffusion distances associated with large fibers.

Similarly, if $SA{:}V$ is lowered to minimize ionic transport costs, then there is no further consequence to lowering aerobic capacity, since high rates of mitochondrial respiration would be limited by low O_2 flux in large fibers.

The implication of the hypothesis that selective pressure to lower maintenance costs favors large fiber size is that the benefits of a rapid aerobic recovery following a burst contraction are outweighed by long-term energetic savings. Blue crabs have large chelipeds and highly effective defensive behavior, and they also have the capacity to rapidly bury themselves to avoid predators. These characteristics may obviate the need for additional high-force contractions following an initial bout of burst swimming and may explain why the juvenile crabs do not also employ anaerobic metabolism to accelerate recovery. Large fibers might be particularly important in reducing metabolic costs in cases where anaerobic muscle constitutes a large fraction of the total body mass and is used infrequently, but must maintain a polarized sarcolemma at all times. Additional examples may include lobster abdominal muscle that is used for tail-flip escape maneuvers, or fish white muscle in species that infrequently undergo burst swimming. At present, however, the benefits of large fiber size, if any, in crustaceans and other groups are not known.

We thank Dr Timothy Moerland for his valuable insights. This research was supported by National Science Foundation grants to S.T.K. (IBN-0316909) and B.R.L. (IBN-0315883).

References

Aliev, M. K. and Saks, V. (1997). Compartmentalized energy transfer in cardiomyocytes: use of mathematical modeling for analysis of in vivo regulation of respiration. *Biophys. J.* **73**, 428-445.

Baldwin, J., Gupta, A. and Iglesias, X. (1999). Scaling of anaerobic energy metabolism during tail flipping behaviour in the freshwater crayfish, *Cherax destructor*. *Mar. Fresh. Res.* **50**,183-187.

Booth, C. E. and McMahon, B. R. (1985). Lactate dynamics during locomotor activity in the blue crab, *Callinectes sapidus*. *J. Exp. Biol.* **118**, 461-465.

Boyle, K. L., Dillaman, R. M. and Kinsey, S. T. (2003). Mitochondrial distribution and glycogen dynamics suggest diffusion constraints in muscle fibers of the blue crab, *Callinectes sapidus*. *J. Exp. Zool.* **297**, 1-16.

Curtin, N. A., Kushmerick, M. J., Wiseman, R. W. and Woledge, R. C. (1997). Recovery after contraction of white muscle fibres from the dogfish, *Scyliorhinus canicula*. *J. Exp. Biol.* **200**, 1061-1071.

de Graaf, R. A., van Kranenburg, A. and Nicolay, K. (2000). *In vivo* ^{31}P-NMR diffusion spectroscopy of ATP and phosphocreatine in rat skeletal muscle. *Biophys. J.* **78**, 1657-1664.

Ellington, W. R. (1983). The recovery from anaerobic metabolism in invertebrates. *J. Exp. Zool.* **228**, 431-444.

Ellington, W. R. (2001). Evolution and physiological roles of phosphagen systems. *Ann. Rev. Physiol.* **63**, 289-325.

Ellington, W. R. and Kinsey, S. T. (1998). Functional and evolutionary implications of the distribution of phosphagens in primitive-type spermatazoa. *Biol. Bull.* **195**, 264-272.

Forgue, J., Legeay, A. and Massabuau, J.-C. (2001). Is the resting rate of oxygen consumption of locomotor muscles in crustaceans limited by the low blood oxygenation strategy? *J. Exp. Biol.* **204**, 933-940.

Gannon, A. T. and Wheatly, M. G. (1995). Physiological effects of a gill barnacle on host blue crabs during short-term exercise and recovery. *Mar. Behav. Physiol.* **24**, 215-225.

Groebe, K. and Thews, G. (1990). Calculated intra- and extracellular gradients in heavily working red muscle. *Am. J. Physiol. Heart Circ. Physiol.* **259**, H84-H92.

Head, G. and Baldwin, J. (1986). Energy metabolism and the fate of lactate during recovery from exercise in the Australian freshwater crayfish, *Cherax destructor*. *Aust. J. Mar. Fresh. Res.* **37**, 641-646.

Henry, R. P., Booth, C. E., Lallier, F. H. and Walsh, P. J. (1994). Post-exercise lactate production and metabolism in three species of aquatic and terrestrial decapod crustaceans. *J. Exp. Biol.* **186**, 215-234.

Hogan, M. C., Stary, C. M., Balaban, R. S. and Combs, C. A. (2005). NAD(P)H fluorescence imaging of mitochondrial metabolism in contracting *Xenopus* skeletal muscle fibers: effect of oxygen availability. *J. Appl. Physiol.* **98**, 1420-1426.

Hubley, M. J., Locke, B. R. and Moerland, T. S. (1997). Reaction–diffusion analysis of effects of temperature on high-energy phosphate dynamics in goldfish skeletal muscle. *J. Exp. Biol.* **200**, 975-988.

Jeneson, J. A. L., Westerhoff, H. V., Brown, T. R., van Echteld, C. J. A. and Berger, R. (1995). Quasi-linear relationship between Gibbs free energy of ATP hydrolysis and power output in human forearm muscle. *Am. J. Physiol. Cell Physiol.* **268**, C1474-C1484.

Jeneson, J. A. L., Wiseman, R. W., Westerhoff, H. V. and Kushmerick, M. J. (1996). The signal transduction function for oxidative phosphorylation is at least second order in ADP. *J. Biol. Chem.* **271**, 27995-27998.

Johnson, L. K., Dillaman, R. M., Gay, D. M., Blum, J. E. and Kinsey, S. T. (2004). Metabolic influences of fiber size in aerobic and anaerobic muscles of the blue crab, *Callinectes sapidus*. *J. Exp. Biol.* **207**, 4045-4056.

Johnston, I. A., Fernández, D. A., Calvo, J., Vieira, V. L. A., North, A. W., Abercromby, M. and Garland, T., Jr (2003). Reduction in muscle fibre number during the adaptive radiation of notothenioid fishes: a phylogenetic perspective. *J. Exp. Biol.* **206**, 2595-2609.

Johnston, I. A., Abercromby, M., Vieira, V. L. A., Sigursteindóttir, R. J., Kristjánsson, B. K., Sibthorpe, D. and Skúlason, S. (2004). Rapid evolution of muscle fibre number in post-glacial populations of charr *Salvelinus alpinus*. *J. Exp. Biol.* **207**, 4343-4360.

Kamp, G. (1989). Glycogenolysis during recovery from muscular work. *Biol. Chem. Hoppe-Swyler.* **370**, 565-573.

Kemp, G. J., Manners, D. N., Clark, J. F., Bastin, M. E. and Radda, G. K. (1998). Theoretical modeling of some spatial and temporal aspects of the mitochondrion/creatine kinase/myofibril system in muscle. *Mol. Cell. Biochem.* **184**, 249-289.

Kinsey, S. T. and Ellington, W. R. (1996). ^{1}H- and ^{31}P-Nuclear magnetic resonance studies of L-lactate transport in isolated muscle fibers from the spiny lobster, *Panulirus argus*. *J. Exp. Biol.* **199**, 2225-2234.

Kinsey, S. T. and Moerland, T. S. (2002). Metabolite diffusion in giant muscle fibers of the spiny lobster, *Panulirus argus*. *J. Exp. Biol.* **205**, 3377-3386.

Kinsey, S. T., Penke, B., Locke, B. R. and Moerland, T. S. (1999). Diffusional anisotropy is induced by subcellular barriers in skeletal muscle. *NMR Biomed.* **11**, 1-7.

Korzeniewski, B. (2003). Regulation of oxidative phosphorylation in different muscles and various experimental conditions. *Biochem. J.* **375**, 799-804.

Mainwood, G. W. and Raukusan, K. (1982). A model for intracellular energy transport. *Can. J. Physiol. Pharmacol.* **60**, 98-102.

Meyer, R. A. (1988). A linear model of muscle respiration explains monoexponential phosphocreatine changes. *Am. J. Physiol*. **254**, C548-C553.

Meyer, R. A., Sweeney, H. L. and Kushmerick, M. J. (1984). A simple analysis of the 'phosphocreatine shuttle.' *Am. J. Physiol.* **246**, C365-C377.

Milligan, C. L., Walsh, P. J., Booth, C. E. and McDonald, D. L. (1989). Intracellular acid-base regulation during recovery from locomotor activity in the blue crab, *Callinectes sapidus*. *Physiol. Zool.* **62**, 621-638.

Morris, S. and Adamczewska, A. M. (2002). Utilisation of glycogen, ATP, and arginine phosphate in exercise and recovery in terrestrial red crabs, *Gecarcoidea natalis*. *Comp. Biochem. Physiol. A*. **133**, 813-825.

Nevo, A. C. and Rikmenspoel, R. (1970). Diffusion of ATP in sperm flagella. *J. Theor. Biol.* **26**, 11-18.

Pate, E. and Cooke, R. (1985). The inhibition of muscle contraction by adenosine 5′ (β, γ-imido) triphosphate and by pyrophosphate. *Biophys. J.* **47**, 773-780.

Rome, L. C. and Lindstedt, S. L. (1998). The quest for speed: muscles built for high-frequency contractions. *News Physiol. Sci.* **13**, 261-268.

Russel, B., Motlagh, D. and Ashley, W. W. (2000). Form follows function: how muscle shape is regulated by work. *J. Appl. Physiol.* **88**, 1127-1132.

Saks, V., Kuznetsov, A., Andrienko, T., Usson, Y., Appaix, F., Guerrero, K., Kaambre, T., Sikk, P., Lemba, M. and Vendelin, M. (2003).

Heterogeneity of ADP diffusion and regulation of respiration in cardiac cells. *Biophys. J.* **84**, 3436-3456.

Schmidt-Nielsen, K. (1984). *Scaling: Why Is Animal Size So Important?* New York: Cambridge University Press.

Smith, E. and Morrison, J. F. (1969). Kinetic studies on the arginine kinase reaction. *J. Biol. Chem.* **244**, 4224-4234.

Stokes, D. R. and Josephson, R. K. (1992). Structural organization of two fast, rhythmically active crustacean muscles. *Cell Tiss. Res.* **267**, 571-582.

Suarez, R. K. (2003). Shaken and stirred: muscle structure and metabolism. *J. Exp. Biol.* **206**, 2021-2029.

Taylor, C. R. and Weibel, E. R. (1981). Design of the mammalian respiratory system. *Respir. Physiol.* **44**, 1-164.

Teague, W. E. and Dobson, G. P. (1999). Thermodynamics of the arginine kinase reaction. *J. Biol. Chem.* **274**, 22459-22463.

Thébault, M. T., Raffin, J. P. and LeGall, J. Y. (1987). In vivo ^{31}P NMR in crustacean muscles: fatigue and recovery in the tail musculature from the prawn, *Palaemon elegans. Biochem. Biophys. Res. Comm.* **145**, 453-459.

Tombes, R. M. and Shapiro, B. M. (1985). Metabolite channeling: a phosphocreatine shuttle to mediate high energy phosphate transport between sperm mitochondrion and tail. *Cell* **41**, 325-334.

Tse, F. W., Govind, C. K. and Atwood, H. L. (1983). Diverse fiber composition of swimming muscles in the blue crab, *Callinectes sapidus*. *Can. J. Zool.* **61**, 52-59.

Tyler, S. and Sidell, B. D. (1984). Changes in mitochondrial distribution and diffusion distances in muscle of goldfish upon acclimation to cold temperatures. *J. Exp. Biol.* **232**, 1-9.

van Dorsten, F. A., Wyss, M., Walliman, T. and Nicolay, K. (1997). Activation of sea urchin sperm motility is accompanied by an increase in the creatine kinase flux. *Biochem. J.* **325**, 411-416.

Vendelin, M., Kongas, O. and Saks, V. (2000). Regulation of mitochondrial respiration in heart cells analyzed by reaction–diffusion model of energy transfer. *Am. J. Physiol. Cell Physiol*. **278**, C747-C764.

Vicini, P. and Kushmerick, M. (2000). Cellular energetics analysis by a mathematical model of energy balance: estimation of parameters in human skeletal muscle. *Am. J. Physiol. Cell Physiol.* **279**, C213-C224.

Walliman, T., Wyss, M., Brdiczka, D., Nicolay, K. and Eppenberger, H. M. (1992). Intracellular compartmentation, structure and function of creatine kinase isoenzymes in tissues with high and fluctuating energy demands: the 'phosphocreatine circuit' for cellular energy homeostasis. *Biochem. J.* **281**, 21-40.

Weisz, P. B. (1973). Diffusion and chemical transformation. *Science* **179**, 433-440.

Zammitt, V. A. and Newsholme, E. A. (1976). The maximum activities of hexokinase, phosphorylase, phosphofructokinase, glycerol phosphate dehydrogenases, lactate dehydrogenase, octopine dehydrogenase, phophoenolpyruvate carboxykinase, nucleoside diphosphatekinase, glutamate-oxaloacetate transaminase, and arginine kinase in relation to carbohydrate utilization in muscles from marine invertebrates. *Biochem. J.* **160**, 447-462.